Article

OPEN ACCESS

THE EMBO JOURNAL

Damage-induced regeneration of the intestinal stem cell pool through enteroblast mitosis in the *Drosophila* midgut

Aiguo Tian[1,2,*], Virginia Morejon[1], Sarah Kohoutek[1], Yi-Chun Huang[1], Wu-Min Deng[1] & Jin Jiang[3]

Abstract

Many adult tissues and organs including the intestine rely on resident stem cells to maintain homeostasis and regeneration. In mammals, the progenies of intestinal stem cells (ISCs) can dedifferentiate to generate ISCs upon ablation of resident stem cells. However, whether and how mature tissue cells generate ISCs under physiological conditions remains unknown. Here, we show that infection of the *Drosophila melanogaster* intestine with pathogenic bacteria induces entry of enteroblasts (EBs), which are ISC progenies, into the mitotic cycle through upregulation of *epidermal growth factor receptor* (EGFR)-Ras signaling. We also show that ectopic activation of EGFR-Ras signaling in EBs is sufficient to drive enteroblast mitosis cell autonomously. Furthermore, we find that the dividing enteroblasts do not gain ISC identity as a prerequisite to divide, and the regenerative ISCs are produced through EB mitosis. Taken together, our work uncovers a new role for EGFR-Ras signaling in driving EB mitosis and replenishing the ISC pool during fly intestinal regeneration, which may have important implications for tissue homeostasis and tumorigenesis in vertebrates.

Keywords dedifferentiation; *Drosophila* midgut; enteroblasts; regeneration; stem cells

Subject Categories Cell Adhesion, Polarity & Cytoskeleton; Development; Stem Cells & Regenerative Medicine

DOI 10.15252/embj.2022110834 | Received 28 February 2022 | Revised 14 July 2022 | Accepted 15 July 2022 | Published online 11 August 2022

The EMBO Journal (2022) 41: e110834

Introduction

The *Drosophila* midgut is the functional equivalent of mammalian small intestine where food is digested and nutrients are absorbed, and the intestinal epithelium protects the internal gut milieu from the external environment (Sansonetti, 2004; Jiang & Edgar, 2012; Li & Jasper, 2016; Zwick *et al*, 2019). During normal homeostasis, both the *Drosophila* midgut and the mammalian small intestine undergo cellular turnover to maintain tissue integrity and function. In response to tissue damage such as feeding with dextran sodium sulfate (DSS) or bacteria, they mount regenerative programs to accelerate stem cell division and differentiation to effectively replenish damaged mature cells (Amcheslavsky *et al*, 2009; Biteau *et al*, 2011; Jiang & Edgar, 2012; Jiang *et al*, 2016). In both mammals and *Drosophila*, the intestinal stem cells (ISCs) divide continuously to give rise to stem cells and progenitor cells, which differentiate into enterocytes (ECs), enteroendocrine (EE) cells (Fig 1A), Paneth cells, tuft cells, or goblet cells (Micchelli & Perrimon, 2006; Ohlstein & Spradling, 2006; Barker *et al*, 2007; Jiang & Edgar, 2012; Beumer & Clevers, 2016; Hung *et al*, 2020). These progenitors from ISCs in mammals enter the trans-amplifying compartment to rapidly divide before terminal differentiation, but the enteroblast (EB) progenitor cells in the *Drosophila* intestine, which undergo endoreplication to become ECs, are not able to proliferate (Micchelli & Perrimon, 2006; Ohlstein & Spradling, 2006, 2007; Beumer & Clevers, 2016). During intestinal regeneration in *Drosophila*, the EGFR-Ras pathway and other signaling pathways, such as the Notch, Wnt, Hh, Insulin, Hippo, JAK–STAT, JNK, and BMP pathways, and the Par complex, are implicated in the regulation of ISC self-renewal, proliferation, and/or differentiation (Micchelli & Perrimon, 2006; Ohlstein & Spradling, 2006, 2007; Biteau *et al*, 2008; Lin *et al*, 2008; Jiang *et al*, 2009, 2011; Buchon *et al*, 2010; Karpowicz *et al*, 2010; Ren *et al*, 2010; Shaw *et al*, 2010; Staley & Irvine, 2010; O'Brien *et al*, 2011; Goulas *et al*, 2012; Biteau & Jasper, 2014; Tian & Jiang, 2014; Beehler-Evans & Micchelli, 2015; Tian *et al*, 2015, 2017; Zeng & Hou, 2015; Chen *et al*, 2018). As a result of activation of EGFR-Ras signaling, ISCs enter mitosis quickly to speed up proliferation and regeneration (Buchon *et al*, 2010; Biteau & Jasper, 2011; Jiang *et al*, 2011). However, whether EGFR-Ras signaling induces EBs to enter mitosis remains unexplored.

In the mammalian intestine, the Dll1^{+} secretory progenitor cells, the mature tuft cells, and Paneth cells undergo dedifferentiation to produce regenerative ISCs after ablation of resident ISCs (van Es *et al*, 2012; Tetteh *et al*, 2016; Schmitt *et al*, 2018; Yu *et al*, 2018;

1 Department of Biochemistry and Molecular Biology, Tulane University School of Medicine, Louisiana Cancer Research Center, New Orleans, LA, USA
2 Tulane Aging Center, Tulane University School of Medicine, New Orleans, LA, USA
3 Department of Molecular Biology and Department of Pharmacology, University of Texas Southwestern Medical Center, Dallas, TX, USA
*Corresponding author. Tel: +15049885315; E-mail: atian@tulane.edu

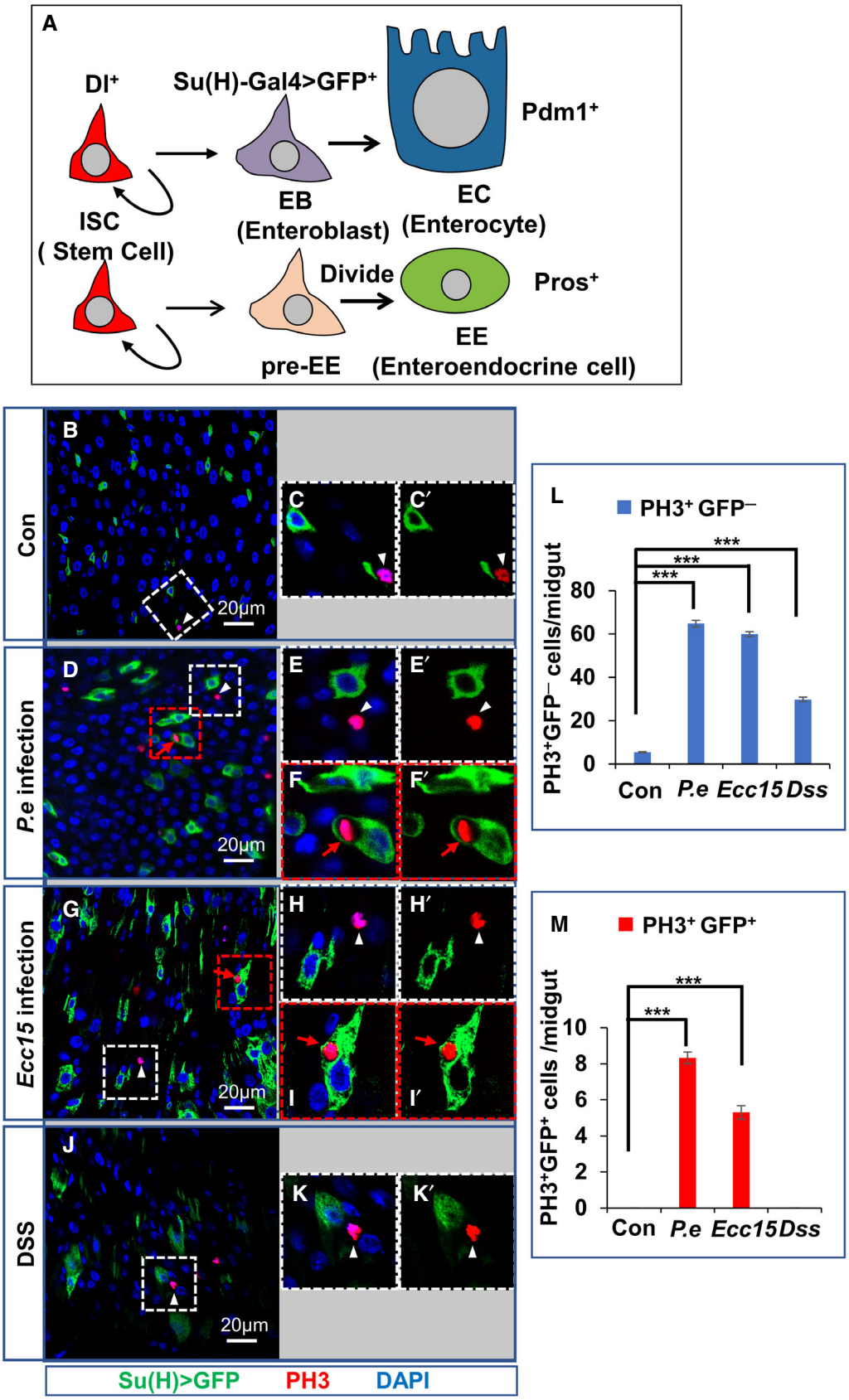

Figure 1.

Figure 1. Bacterial infection can induce EB mitosis.

A ISC lineages in *Drosophila* adult midguts. Dl marks ISCs. *Su(H)-Gal4>UAS-CD8:GFP* marks EBs. Pdm1 and Prospero (Pros) are markers for EC and EE, respectively.

B–K′ The *Drosophila* posterior midguts containing *Su(H)-Gal4>UAS-CD8:GFP* (*Su(H)>GFP*) with sucrose (Suc, control) (B–C′), *P.e.* for 36 h (D–F′), *Ecc15* for 36 h (G–I′), and DSS for 36 h (J–K′) were immunostained for GFP (green), PH3 (red), and DAPI (blue). (C, C′, E, E′, H, H′ and K, K′) Magnification of selected areas containing $PH3^+GFP^-$ cells from B, D, G, and J. The EB cell close to the $PH3^+$ cell (white arrow) in C, C′ is out of focus. (F, F′, I and I′) Magnification of selected areas containing $PH3^+$ EBs (GFP^+) from D and G. White arrowheads and red arrows indicate PH3 in GFP^- and GFP^+ cells, respectively.

L, M Quantification of $PH3^+GFP^-$ ISCs (L) and $PH3^+GFP^+$ EBs (M) with given treatments. $n = 21$ guts for each treatment.

Data information: Three independent experiments were performed, and error bars are ±SEM. ***$p < 0.001$ (Student's *t*-test) (L, M).

Jones *et al*, 2019; Murata *et al*, 2020). By contrast, in *Drosophila* midguts, the differentiating ECs were found to produce regenerative ISCs through amitosis in the re-feeding condition in starved midguts (Lucchetta & Ohlstein, 2017). The EB progenitor cells, which normally enter endoreplication to become ECs, have been shown to re-enter the mitotic cycle upon *P.e.* infection or with misexpression of cell cycle genes such as Cdc25 phosphatase *string (stg)* and *CycE*, or loss of a CDK1 inhibitory kinase *Myt1* (Kohlmaier *et al*, 2015; Willms *et al*, 2020). However, the mechanisms through which EBs enter mitosis in response to *P.e.* infection and whether EB mitosis produces regenerative ISCs remain unclear.

In this study, we find that EBs enter the mitotic cycle during intestinal regeneration in response to bacterial infection through activation of EGFR-Ras signaling. We show that activation of EGFR-Ras signaling in EBs is sufficient to induce EB mitosis. Following the lineages of EBs with the Flp-out and two-color lineage tracing systems, we show that the regenerative stem cells are produced through EB mitosis. Furthermore, we provide evidence to show that these regenerative stem cells are multipotent.

Results

Bacterial infection induces EBs to enter mitosis

To determine whether EBs enter the mitotic cycle upon infection of multiple bacterial strains, adult female flies were fed with pathogenic bacteria (*Pseudomonas entomophila*, *P.e.*, or *Erwinia carotovora carotovora* strain *15*, *Ecc15*) for 36 h (h), and mitosis in their midguts was examined by immunostaining for the mitotic marker PH3 (phospho-Ser10-Histone H3). The EBs were marked by expression of *UAS-GFP* driven by the EB-specific Gal4 (*Su(H)-Gal4*) (Zeng *et al*, 2010) (*Su(H)-Gal4>UAS-CD8:GFP* is referred to as *Su(H)>GFP*) (Fig 1A). Adult female flies fed with sucrose (Suc) were used as the control. In midguts of adult female flies fed with *P.e.* or *Ecc15*, the number of the mitotic cells ($PH3^+$) without GFP expression (i.e., ISCs) ($PH3^+GFP^-$ cells) (Fig 1D–E′ and G-H′, white arrowheads) was significantly increased when compared with those in the control (Fig 1B–C′) (Fig 1L: 64.8 PH3/gut in *P.e.* infection vs. 59.95 PH3/gut in *Ecc15* infection vs.5.5 PH3/gut in the control; $n = 21$), similar to what was reported previously (Buchon *et al*, 2009; Jiang *et al*, 2011). Interestingly, PH3 staining was present in some EBs (GFP positive) in *P.e.* infected midguts ($PH3^+GFP^+$, Fig 1D, F and F′, red arrows), as previously reported (Kohlmaier *et al*, 2015), or in *Ecc15*-infected midguts ($PH3^+GFP^+$, Fig 1G, I and I′, red arrows), but not in control midguts (Fig 1B) (Fig 1M: 8.33 PH3/gut in *P.e.* vs. 5.3 PH3/gut in *Ecc15* vs. 0 PH3/gut in the control, $n = 21$), suggesting that bacterial infection prevents some EBs to enter the endoreplication cycle, and induces them to enter the mitotic cycle. The entry into mitosis in EBs in response to *P.e.* or *Ecc15* infection suggests that pathogenic bacterial infection has a general effect on triggering EB mitosis in the adult midguts. In contrast, in the midguts of flies fed with dextran sodium sulfate (DSS) or Bleomycin (Bleo), which induces ISC proliferation (Amcheslavsky *et al*, 2009; Ren *et al*, 2013; Tian *et al*, 2015), PH3 signal was found only in ISCs without GFP expression (DSS: 29.8 PH3/gut, $n = 21$, Fig 1J–L. Bleo: 55.2 PH3/gut, $n = 21$, Fig EV1A), but not in EBs with GFP expression (Figs 1J and M, and EV1A).

To ascertain that EBs indeed underwent mitosis upon bacterial infection, we examined the expression of Delta (Dl), an ISC marker, and found that the dividing ISCs without GFP expression ($PH3^+GFP^-$) showed Dl expression (Fig 2A–A″ and C–C″, white arrows), but these dividing EBs ($PH3^+GFP^+$) did not gain Dl expression ($GFP^+PH3^+Dl^-$, Fig 2B–B″, red arrows, 100%, $n = 89$), suggesting that both EBs and ISCs enter mitosis upon bacterial infection. We performed additional experiments to examine EB mitosis in which ISCs were marked by the expression of *UAS-GFP* driven by *esgGal4*, *su(H)-Gal80*. Adult female flies with *esgGal4*, *su(H)-Gal80>UAS-GFP* were fed with Suc, *P.e.* bacteria or Dss, and their intestines were dissected out for immunostaining with anti-GFP, PH3, and Pros (the EE cell marker) antibodies. We found PH3 in GFP^+ ISCs in all conditions (Fig 2D–F″, white arrows). However, PH3 expression was present in EBs marked by $Pros^-$ GFP^- and small nuclei only upon *P.e.* infection (Fig 2E–E″, red arrows, G), but

Figure 2. Dividing EBs do not gain Dl expression.

A–C″ The midguts from the adult female flies fed with Suc (control) (A–A″), *P.e.* (B–B″) or DSS (C–C″) were immunostained with anti-PH3 and anti-Dl antibodies. The white arrows indicate that GFP^- cells with PH3 have Dl staining and the red arrows indicate that EBs with GFP and PH3 (GFP^+PH3^+) do not have Dl expression. The yellow arrows in B show that two ISCs with PH3 are out of focus.

D–F″ When the ISCs were marked by *esgGal4*, *su(H)-Gal80>UAS-GFP*, PH3 expression was found in GFP^+ ISCs with feeding of Suc (control) (D–D″), *P.e.* (E–E″) and Dss (F–F″). However, PH3 expression is present in EBs with GFP^-Pros^- and small nuclei upon *P.e.* infection (E–E″, red arrows). The white arrows indicate GFP^+ cells with PH3 expression.

G Quantification of $PH3^+GFP^-Pros^-$ EBs with given treatments. $n = 11$ guts for each treatment. Data information: Three independent experiments were performed, and error bars are ±SEM. ***$p < 0.001$ (Student's *t*-test) (G).

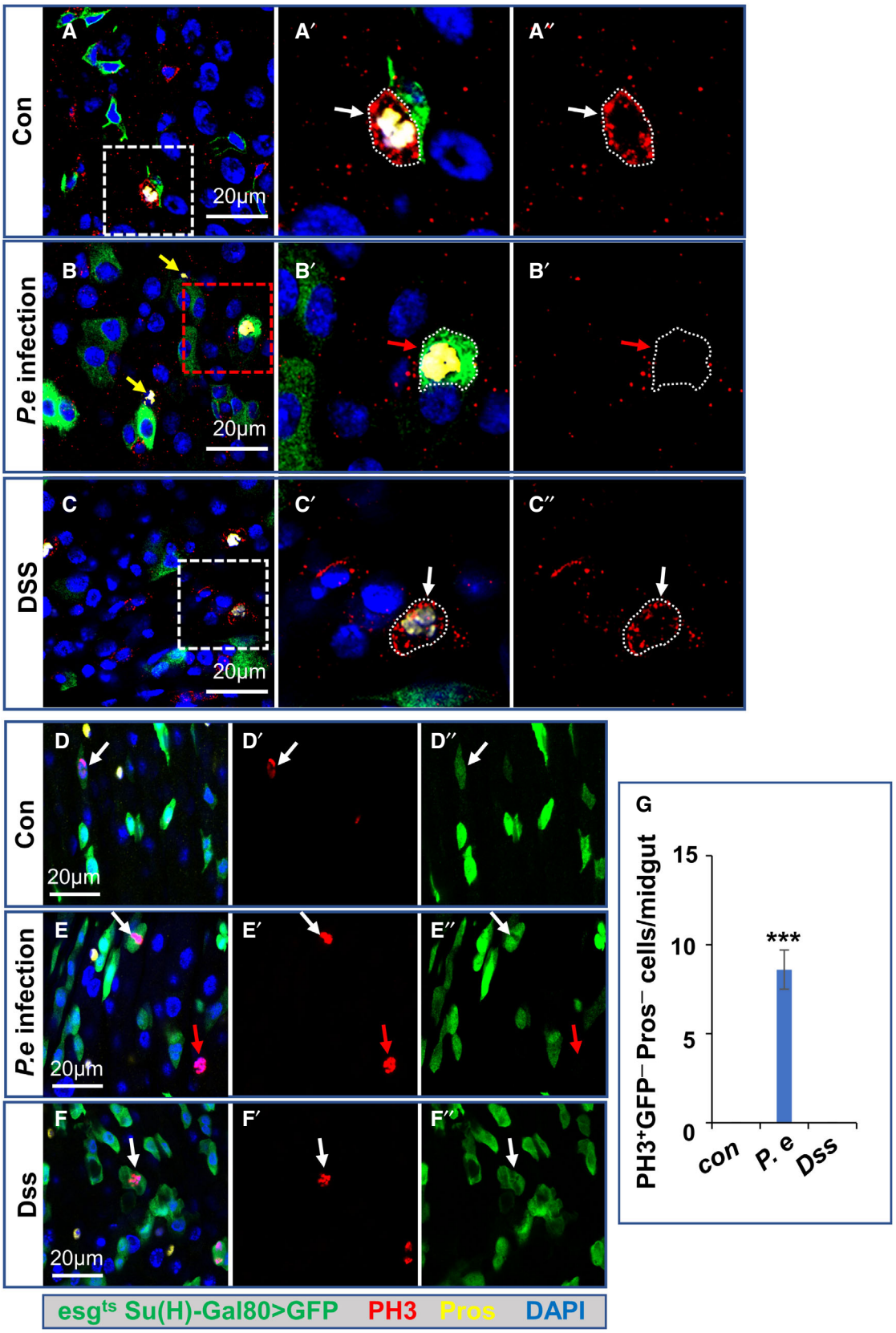

Figure 2.

not upon Suc and Dss feeding. We also knocked down *stg*, the Cdc25 phosphatase that activates the mitotic kinase CDK1, in EBs with *su(H)^{ts}>UAS-stg-RNAi* and examined whether EB mitosis was blocked in response to *P.e.* infection. The number of EBs with PH3 expression was significantly reduced compared with intestines without *stg* knockdown (Fig EV1B). These results confirmed that EBs can enter the mitotic cycle upon bacterial infection.

In response to *P.e.* infection, both ISCs and EBs can enter mitosis, therefore we wonder whether EB mitosis and ISC mitosis are compensatory. To test this, we blocked ISC proliferation by expressing *UAS-stg-RNAi* with *Dl-Gal4^{ts}* and examined EB mitosis upon *P.e.* infection. We found that expression of *stg* in ISCs significantly reduced overall PH3$^+$ cell number (Fig 3A). Quantification of mitotic EBs (PH3$^+$GFP$^-$Pros$^-$) revealed a slight reduction rather than increase in EB mitosis when ISC proliferation was blocked (Fig 3B), indicating that EB mitosis does not act as a compensatory mechanism for ISC mitosis upon injury.

EGFR-Ras signaling in EBs is required and sufficient to induce EB mitosis

Bacterial infection activates several signaling pathways including the EGFR-Ras pathway through up-regulation of ligands to induce ISC proliferation (Jiang *et al*, 2011). To assess the expression level of ligands of the EGFR-Ras pathway, we performed qRT-PCR analysis and found that *P.e.* infection increased the expression of ligands *vein* (*vn*) and *Keren* (*Krn*) (Fig 4A). In addition, we examined the activity of mitogen-activated protein kinase (MAPK) in EBs, which marks the activity of EGFR-Ras signaling, by using an antibody against the diphosphorylated and active form of MAPK (dpERK) (Gabay *et al*, 1997). Without *P.e.* infection, the dpErk level was high in ISCs (GFP$^-$, Fig 4B–B″, yellow arrowheads) but low in EBs (GFP$^+$, Fig 4B–B″, white arrows) (Jiang *et al*, 2011). Upon *P.e.* infection, the level of dpERK was greatly increased in both EBs (Fig 4C–C″, white arrows) and ISCs (Fig 4C–C″, yellow arrowheads), suggesting that EGFR-Ras signaling was up-regulated in both EBs and ISCs upon bacterial infection.

To determine whether activation of EGFR-Ras signaling induces EBs to enter the mitotic cycle, we overexpressed the active form of *Ras* (*UAS-Ras^{V12}*) (Karim & Rubin, 1998) with the EB-specific inducible Gal4/Gal80^{ts} system (*Su(H)-Gal4 Tub-Gal80^{ts}*; referred to as *Su(H)^{ts}*) and examined the expression of the mitotic marker (PH3). In the experiments with Gal80^{ts}, female flies expressing *Su(H)^{ts}>UAS-CD8:GFP* with or without *UAS – gene* were raised to adults at 18°C (Gal4 is 'off') and then shifted to 29°C to degrade Gal80^{ts} (Gal4 is 'on') so that *Su(H)-Gal4* can drive expression of *UAS-gene*. Our assay with expression of *Ras^{V12}* in EBs showed that activation of *Ras* in EBs induced cell-autonomous EB mitosis (GFP$^+$ PH3$^+$, Fig 4F, H and H′, red arrows; Fig 4O: 12.7 PH3/gut in *Ras^{V12}* vs. 0 PH3/gut in the control (Fig 4D), $n = 13$). In addition, we found that activation of *Ras* in EBs promoted ISC proliferation noncell-autonomously (PH3$^+$ GFP$^-$, Fig 4F–G′, arrowheads, Fig 4P: 27.8 PH3/gut in *Ras^{V12}* vs. 5.4 PH3/gut in the control (Fig 4D–E′), $n = 13$), indicated by increased number of PH3 in GFP$^-$ ISCs. To confirm that EGFR-Ras signaling induces EB mitosis, we used the same EB-specific *Gal4/Gal80^{ts}* system (*Su(H)^{ts}*) to overexpress the active forms of *EGFR* (*EGFR^{A887T}* and *λTop*) (Queenan *et al*, 1997; Lesokhin *et al*, 1999) in EBs, and found that overexpression of either *EGFR^{A887T}* or *λTop* induced EB mitosis (PH3$^+$GFP$^+$; Fig 4I, K, K′, L, N and N′, red arrows, Fig 4O: 9.9 PH3/gut in *EGFR^{A887T}* vs. 6.6 PH3/gut in *λTop* vs. 0 PH3/gut in the control, $n = 13$) and increased ISC mitosis noncell-autonomously (GFP$^-$ PH3$^+$, Fig 4I–J′ and L–M′, arrowheads, Fig 4P). As a control, we used *Su(H)^{ts}* to drive expression of an active form of *InR* (*UAS-InR^{ACT}*) in EBs and the PH3 signal was detected in ISCs but was not detected in EBs (Fig EV1C).

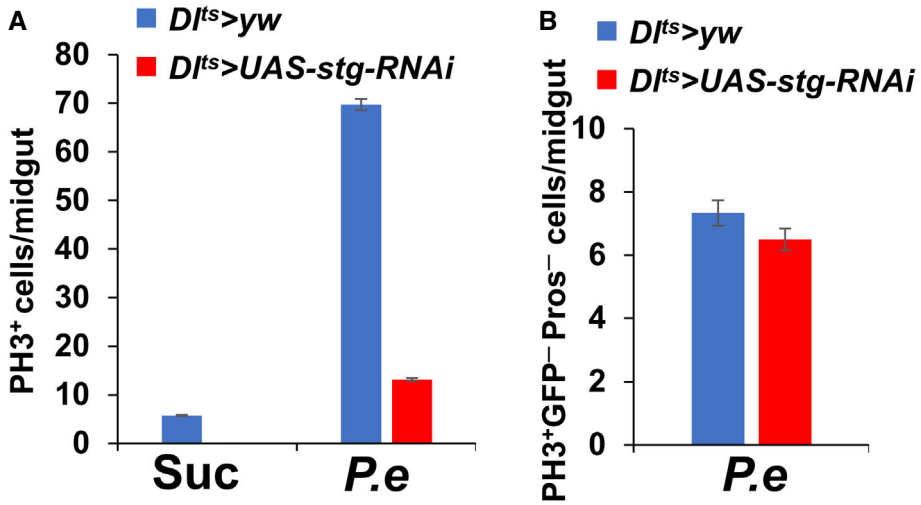

Figure 3. The EB mitosis is not compensatory for ISC mitosis in response to *P.e.* infection.

A Quantification of PH3$^+$ cells when the ISC mitosis was blocked by expressing *stg-RNAi* in ISCs with feeding of Suc or *P.e.* $n = 10$ guts for each treatment.

B Quantification of PH3$^+$ EBs (GFP$^-$Pros$^-$) with or without *stg* expression in ISCs upon *P.e.* infection. $n = 10$ guts for each treatment.

Data information: Three independent experiments were performed.

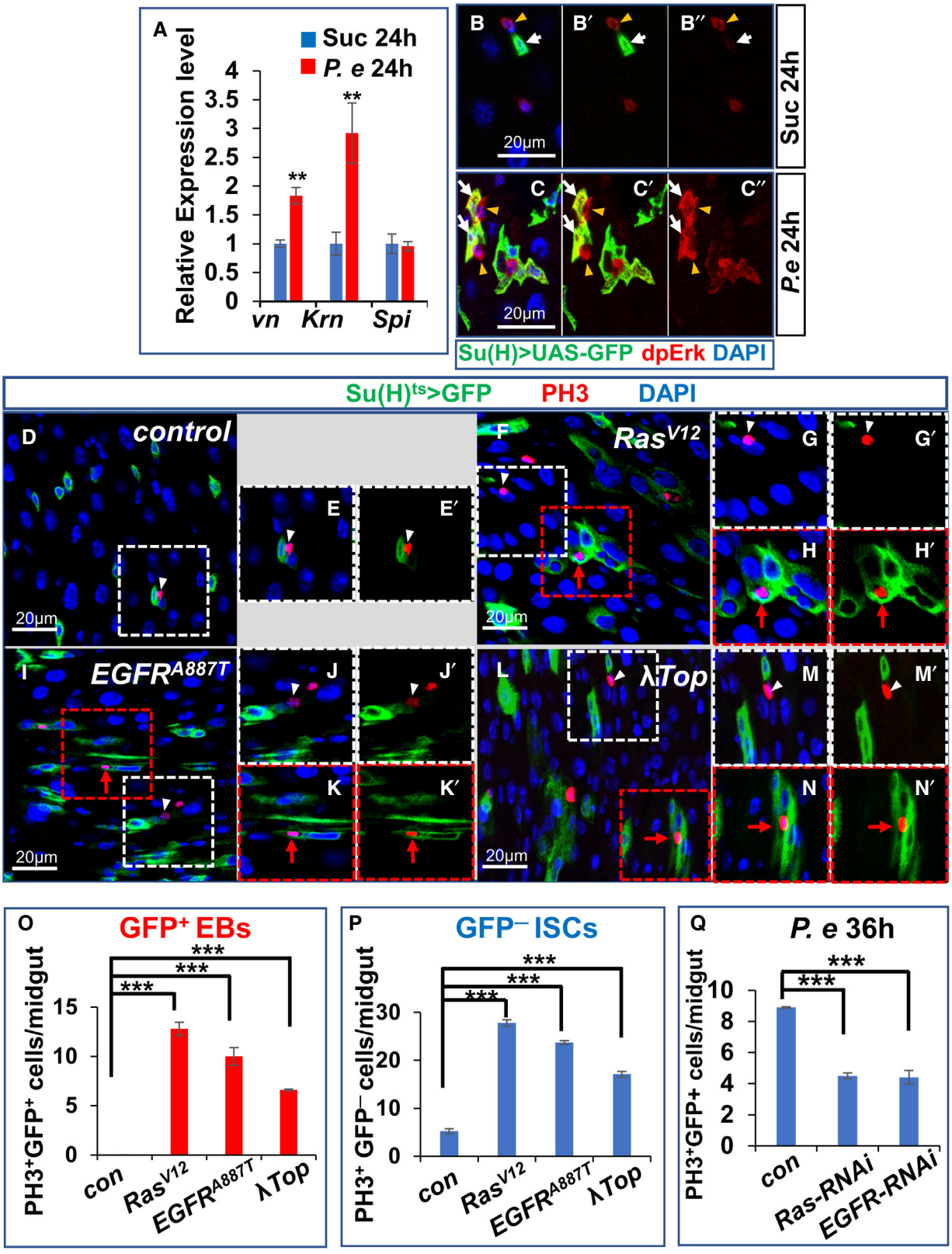

Figure 4.

Figure 4. Activation of EGFR-Ras signaling in EBs is sufficient and required to induces cell-autonomous EB mitosis.

A *P.e.* infection up-regulates the expression of EGFR ligands (*un* and *Krn*).

B–B″ In the control, the dpErk level is high in ISCs (yellow arrowheads), but low in EBs (white arrows).

C–C″ The level of dpErk is greatly up-regulated in both EBs (white arrows) and ISCs (yellow arrowheads) upon bacterial infection.

D–N′ The *Drosophila* midguts expressing *Su(H)^{ts}>GFP* with control (D–E′), *UAS-Ras^{V12}* for 6 days (F–H′), *EGFR^{A887T}* for 4 days (I–K′), and *UAS-λTop* for 5 days (L–N′) were immunostained for GFP (green), PH3 (red) and DAPI (blue). (E, E′, G, G′, J, J′, M, and M′) Magnification of selected areas containing PH3$^+$GFP$^-$ cells from D, F, I and L. (H, H′, K, K′, N, and N′) Magnification of selected areas containing PH3$^+$GFP$^+$ cells from F, I, and L. White arrowheads and red arrows indicate PH3 in GFP$^-$ ISCs and GFP$^+$ EBs, respectively.

O, P Quantification of PH3$^+$GFP$^-$ (P) and PH3$^+$GFP$^+$ (O) in midguts with indicated genotypes. n = 13 guts for each genotype.

Q Quantification of PH3$^+$ EBs (GFP$^+$) with the given genotypes in response to *P.e.* infection. n = 11 guts for each genotype.

Data information: Three independent experiments were performed, and error bars are ±SEM. $^{**}p < 0.01$ (Student's *t*-test) (A). $^{***}p < 0.001$ (Student's *t*-test) (O—Q).

As *P.e.* infection up-regulated EGFR-Ras signaling and activation of EGFR-Ras signaling induced EB mitosis, we asked whether EGFR-Ras signaling was required for EB mitosis in response to *P.e.* infection. To this end, we inactivated EGFR-Ras signaling in EBs by knocking down either *EGFR* or *Ras* with *UAS-EGFR-RNAi* (or *UAS-Ras-RNAi*) driven by *Su(H)^{ts}* (referred to as *Su(H)^{ts}>EGFR-RNAi* (or *Su(H)^{ts}>Ras-RNAi*)) and analyzed the mitotic marker in the EBs upon *P.e.* infection. The knockdown of either *EGFR* or *Ras* decreased the frequency of EB mitosis, as indicated by the reduced number of EBs with PH3 signal (PH3$^+$ GFP$^+$, Fig 4Q: 8.9 PH3/gut in control vs. 4.5 PH3/gut in *EGFR-RNAi* vs. 4.4 PH3/gut in *Ras-RNAi*; n = 11), indicating that EGFR-Ras signaling in EBs is required for EB mitosis upon bacterial infection.

To determine whether the GFP$^+$ EBs gain ISC identity as a prerequisite to divide, we analyzed the expression of Dl, the ISC marker, in midguts with *EGFR^{A887T}* expression. In contrast to the ISCs that showed expression of both PH3$^+$ and Dl (Fig 5A–A″, white arrows), the dividing EBs (GFP$^+$) did not possess Dl expression (Fig 5B–B″, red arrows; 100%, n = 42), suggesting that these EBs do not gain ISC identity. In summary, activation of EGFR-Ras signaling in EBs induces cell-autonomous EB mitosis and promotes ISC proliferation noncell-autonomously.

To further characterize EB mitosis, we examined the phases of mitosis in EBs and ISCs with the mitotic marker PH3 and the centrosome marker Cnn-GFP. Different phases of mitosis such as prophase, metaphase and anaphase were found in dividing EBs (Fig 5F–N), as were detected in ISCs (Fig 5C–E), suggesting normal mitosis in EBs, but difference from the amitosis (Lucchetta & Ohlstein, 2017).

P.e. infection induces EBs to generate Dl$^+$ ISC-like cells through EGFR-Ras signaling

To determine the cell fate of the progenies of EB mitosis, we used the Flip-out lineage tracing system (Fig 6A; Golic & Lindquist, 1989; Germani *et al*, 2018). In this system, *Su(H)-Gal4* driven flippase (Flp) induces the removal of the "stop cassette" in *actP (FRT Stop FRT) LacZ* (referred to as *actP>stop>lacZ)*, thus *LacZ* is expressed to mark the EBs and their progenies. For lineage tracing of control flies fed with Suc, the GFP$^+$ EBs were labeled with *LacZ* expression (*Dl$^-$GFP$^+$LacZ$^+$*, Fig 6B–B‴, white arrows), whereas *LacZ* expression was absent in the ISCs (*Dl$^+$ GFP$^-$*, Fig 6B–B‴, blue arrowheads). In contrast, after feeding with *P.e.*, *LacZ* expression was not only found in GFP$^+$ EBs (Fig 6C–C‴, white arrows), but also in some GFP$^-$ cells (Fig 6C–C‴, red arrowheads). The expression of *LacZ* but lack of GFP suggests that these cells are progenies of EBs but are different from the EB fate. In some of these *LacZ$^+$GFP$^-$* cells, Dl expression was detected (Fig 6C–C‴, red and blue arrowheads, Fig 6D), suggesting that these EB progeny cells may have adopted an ISC-like fate upon *P.e.* infection. In addition, some EBs (GFP$^+$) without *LacZ* expression had been found due to quick regeneration of EBs from ISCs (Fig 6C).

To determine whether the generation of new Dl$^+$ ISC-like cells from EBs upon *P.e.* infection depends on EGFR-Ras signaling, we knocked down *EGFR* in EBs using the Flp-out system. We found that the total number of regenerative Dl$^+$ cells from EBs in response to *P.e.* infection was reduced when *EGFR* was knocked down (total number of *GFP$^-$LacZ$^+$Dl$^+$* cells in five midguts: 28.5 in *P.e.* infection vs. 11.3 in *EGFR-RNAi* with *P.e.* infection, Fig 6E), indicating that EGFR-Ras signaling is required for generation of Dl$^+$ ISC-like cells from EBs.

Activation of EGFR-Ras signaling in EBs is sufficient to drive EBs to produce dl$^+$ ISC-like cells

To determine whether activation of EGFR-Ras signaling in EBs is sufficient to induce EBs to produce Dl$^+$ ISC-like cells, we used the same *Su(H)-Gal4*-driven Flip-out lineage tracing system to express *UAS-Ras^{V12}* in EBs and compared it with the control (Fig 7A–A‴). We found that *LacZ* expression was detected in EB cells (*GFP$^+$LacZ$^+$*, Fig 7B–B‴, white arrows) and their progeny (*GFP$^-$LacZ$^+$*, Fig 7B–B‴, red arrowheads) upon *Ras^{V12}* expression. In addition, we found that some EB progeny cells (*LacZ$^+$GFP$^-$*) exhibited Dl expression (*GFP$^-$LacZ$^+$Dl$^+$*) (Fig 7B–B‴, red and blue arrowheads, and Fig 7D), indicating that activation of EGFR-Ras signaling in EBs is sufficient to induce EBs to generate Dl$^+$ ISC-like cells.

New ISCs are generated through EB division

To confirm that the EB progeny cells with Dl expression are generated from the mitotic divisions, we blocked EB mitosis by knocking down *stg* and examined whether the new Dl$^+$ ISC-like cells were still generated from EBs. To this end, we co-expressed *Ras^{V12}* and *stg-RNAi* in EBs with the *Su(H)-Gal4*-driven Flip-out system and examined the lineages from EBs. We found that the frequency of new Dl$^+$ ISC-like cells (LacZ$^+$GFP$^-$ cells) was significantly reduced (Fig 7C and D), suggesting that the generation of new Dl$^+$ ISC-like cells is suppressed by inhibiting EB mitosis.

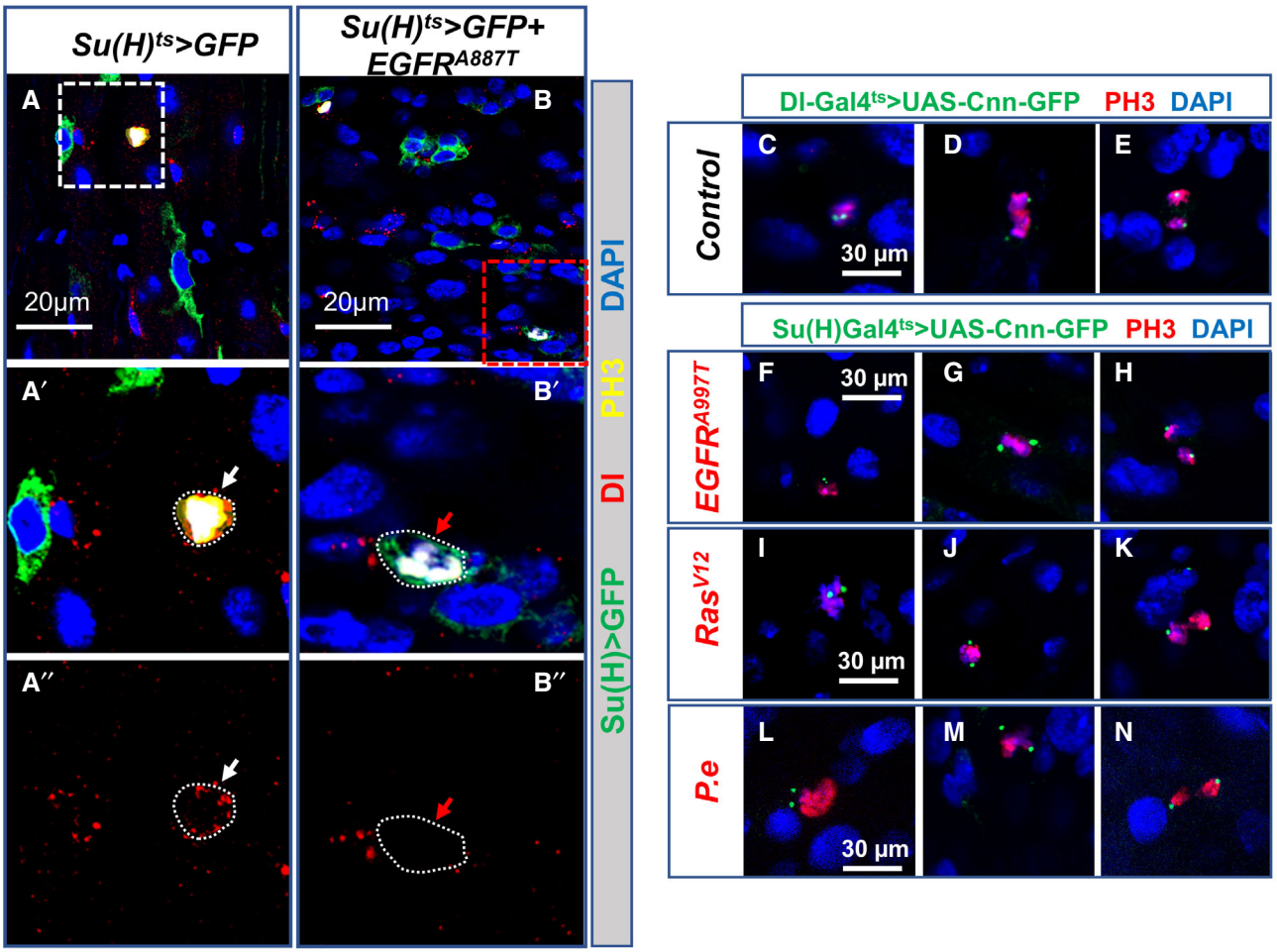

Figure 5. Activation of EGFR-Ras signaling in EBs induces EB mitosis.

A–B″ PH3 and Dl staining in the control (A–A″) or midguts with *EGFR*^{A887T} overexpression (B–B″). The white arrows indicate that GFP^{-} ISCs with PH3 have Dl staining (A–B″); the red arrows indicate that GFP^{+} EBs with PH3 (GFP^{+}PH3^{+}) do not have Dl expression (B–B″).

C–E The different mitotic phases in ISCs with PH3 and the centrosome marker (Cnn-GFP) with *Dl-Gal4> UAS-Cnn-GFP*.

F–N The different mitotic phases in EBs with PH3 and Cnn-GFP when *EGFR*^{A887T} (F–H) or *Ras*^{V12} (I–K) is expressed in EBs with *Su(H)-Gal4* or these flies were fed with *P.e.* (L–N).

Next, we directly marked two cells from one EB division and characterized the two cells by using the two-color lineage tracing system (Fig 8A and B). This system is based on the mitotic division of cells, thus only cells from EB division will be marked by the single color (GFP or RFP). After the single-color clones are produced and the number of cells in single-color clones is counted, we can determine whether the cells from EBs are ISCs (Fig 8B). In this experiment, 3–5-day-old flies expressing *UAS-Flp; Su(H)*^{ts}*; FRT82BGFP/FRT82BRFP* with or without *UAS-EGFR*^{A887T} raised in 18°C were transferred to 29°C for 5 days and these pairs of single-color clones with GFP or RFP in the midguts were analyzed. We found that pairs of single-color clones were produced in midguts with activation of *EGFR-Ras* signaling by *UAS-EGFR*^{A887T} expression (Figs 8D–D″ and F, and EV2), but not in the control midguts (Fig 8C–C″ and F). This result indicates that EBs with *EGFR*^{A887T} expression underwent mitosis, but EBs in the control did not. Interestingly, after the number of cells in single-color clones was counted, we found that the clones in most of pairs of single-color clones had more than one cell (Fig 8D–D″ and F), indicating that EBs underwent symmetric cell division to produce two ISCs. In addition, we found low frequency of clones with asymmetric cell division, as indicated by one clone with one cell and the other clone with multiple cells in the pair of single-color of clones (Figs EV2B–B″ and 8F), or with symmetric non-ISC division, as marked by only one cell in each of the pair of single-color of clones (Figs EV2A–A″ and 8F). Then, we examined the progenies of EBs and the division pattern of EBs in response to *P.e.* infection with the two-color lineage tracing system. After feeding with *P.e.* for 36 h and normal food for 24 h, single-color clones were found (Fig 8E–E″ and F), and there was more than one cell in most of the pairs of single-color clones (Fig 8F). In summary, the results indicate that both activation of EGFR-Ras signaling and bacterial infection induce EBs to generate ISCs through mitosis.

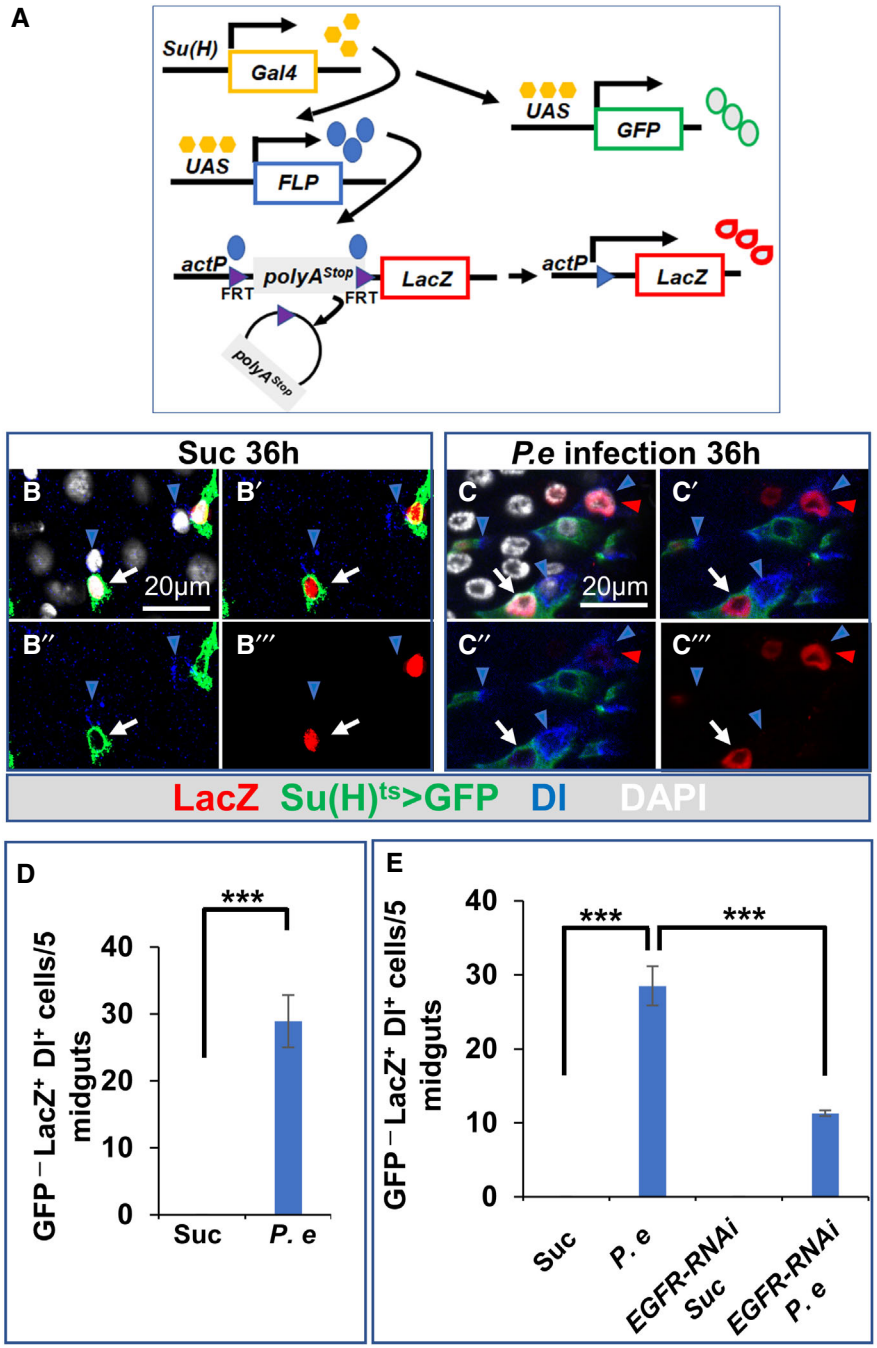

Figure 6. Dl$^+$ ISC-like cells are generated from EBs upon *P.e.* infection.

A The schematic drawing of the Flip-out lineage tracing system.

B–C‴ Flies expressing UAS-Flp; Su(H)ts UAS-CD8:GFP; ActP>Stop>LacZ were fed with Suc (B, B‴) or *P.e.* (C, C‴) for 36 h and their midguts were dissected and immunostained with antibodies against GFP, β-gal and Dl. Blue arrowheads indicate Dl+ ISCs; white arrows indicate GFP+ EBs; and red arrowheads indicate EB progeny cells (LacZ+GFP−).

D Quantification of Dl$^+$ ISC-like cells from EBs (GFP−LacZ$^+$Dl$^+$) in the control, *P.e.* infected midguts, $n = 50$.

E Quantification of Dl$^+$ ISC-like cells from EBs (GFP−LacZ$^+$Dl$^+$) in the control with Suc or *P.e.*, or knockdown of EGFR with Suc or *P.e.* infection, $n = 50$.

Data information: Three independent experiments were performed, and error bars are ±SEM. ***$p < 0.001$ (Student's *t*-test) (D, E).

The single-color clones with more than one cell indicate that new cells from EB mitosis are ISCs which can self-renew and divide. Our next question is whether the new ISCs from EBs can differentiate into mature cells (EE cells or ECs). To test this, we first examined whether the progenies from EBs can differentiate into EE cells or pre-EE cells with an EE marker, Prospero (Pros). When we

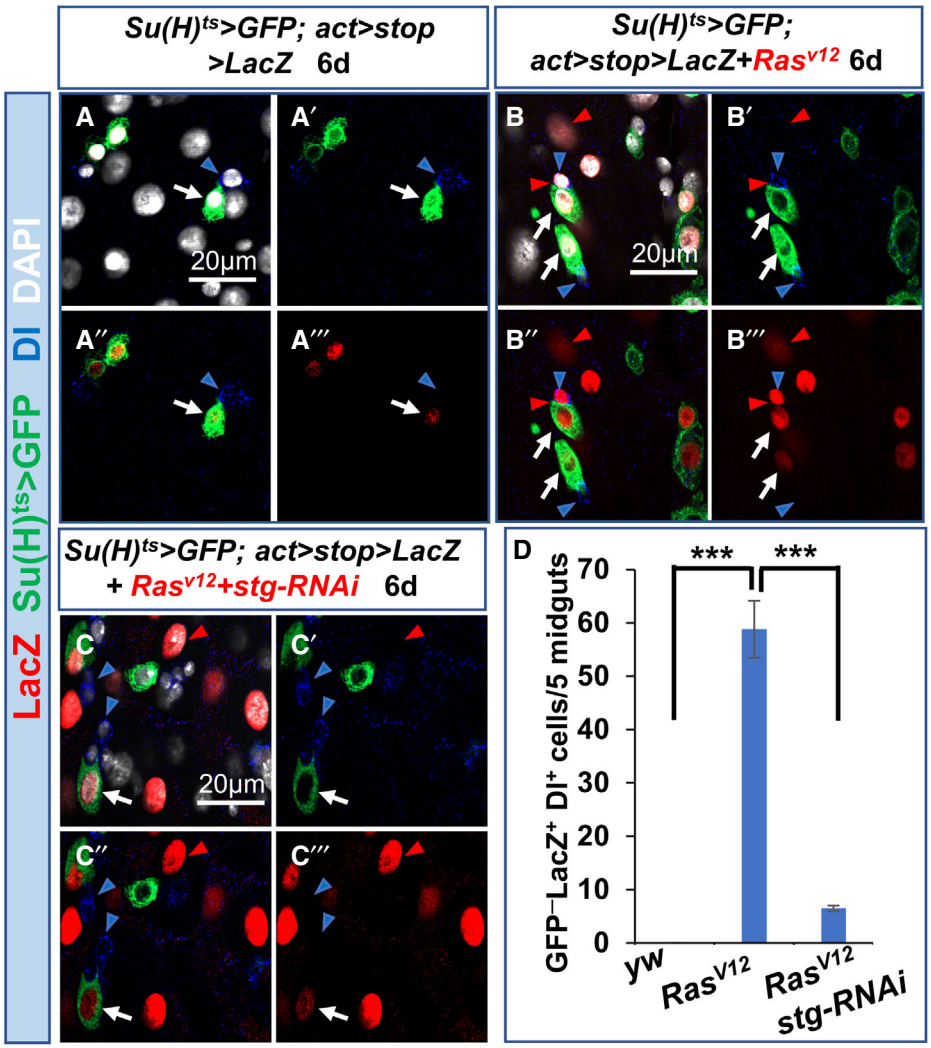

Figure 7. Activation of EGFR-Ras signaling in EBs induces EBs to produce Dl.$^+$ ISC-like cells

A–C‴ The midguts from adult female flies expressing *UAS-Flp; Su(H)^{ts} UAS-CD8:GFP; ActP>Stop>LacZ* with (B–B‴) or without (A–A‴) *UAS-Ras^{V12}* or with *UAS-Ras^{V12}* and *UAS-stg-RNAi* (C–C‴) were dissected and immunostained with antibodies against GFP, β-gal and Dl. The bigger GFP$^-$ nucleus with LacZ expression (only red arrowheads) indicate differentiating or mature ECs. Blue arrowheads indicate Dl$^+$ ISCs; white arrows indicate GFP$^+$ EBs; and red arrowheads indicate EB progeny cells (LacZ$^+$GFP$^-$).

D Quantification of Dl$^+$ ISC-like cells from EBs (*GFP$^-$LacZ$^+$Dl$^+$*) in the indicated genotypes, $n = 50$.

Data information: Three independent experiments were performed, and error bars are ±SEM. ***$p < 0.001$ (Student's *t*-test) (D).

performed the Flp-out lineage tracing experiments with activation of EGFR-Ras signaling or *P.e.* infection and immunostaining with the antibody against Pros and compared them with the control (Fig 9A–A″), we found that some EB progeny cells without GFP expression (*LacZ$^+$GFP$^-$*) have Pros expression (Fig 9B–D), indicating that these ISCs from EBs are functional to generate pre-EE or EE cells. Second, we examined whether the progenies from EBs can differentiate into ECs with an EC marker (Pdm1). Because the Flp-out lineage tracing system cannot distinguish between ECs from original EBs and ECs from the regenerative ISC-EBs, we examined single-color clones with multiple cells upon *EGFR^{A887T}* expression or *P.e.* infection with the EC marker (Pdm1). We found that the Pdm1 signal were identified in the single-color clones (Fig 9E–F″, 100% in single-color clones with multiple cells, $n = 31$), indicating that the new ISCs from EB mitosis can differentiate into mature ECs. Taken together, these results suggest that the regenerative ISCs from EBs are multipotent and functional.

Discussion

Previous studies found that only resident ISCs in *Drosophila* midguts localized at the basal side of the gut epithelium undergo asymmetric cell division to produce renewed ISCs and EBs (Micchelli & Perrimon, 2006; Ohlstein & Spradling, 2006). Our studies show that EBs can generate functional stem cells (Fig 9G), and there are two

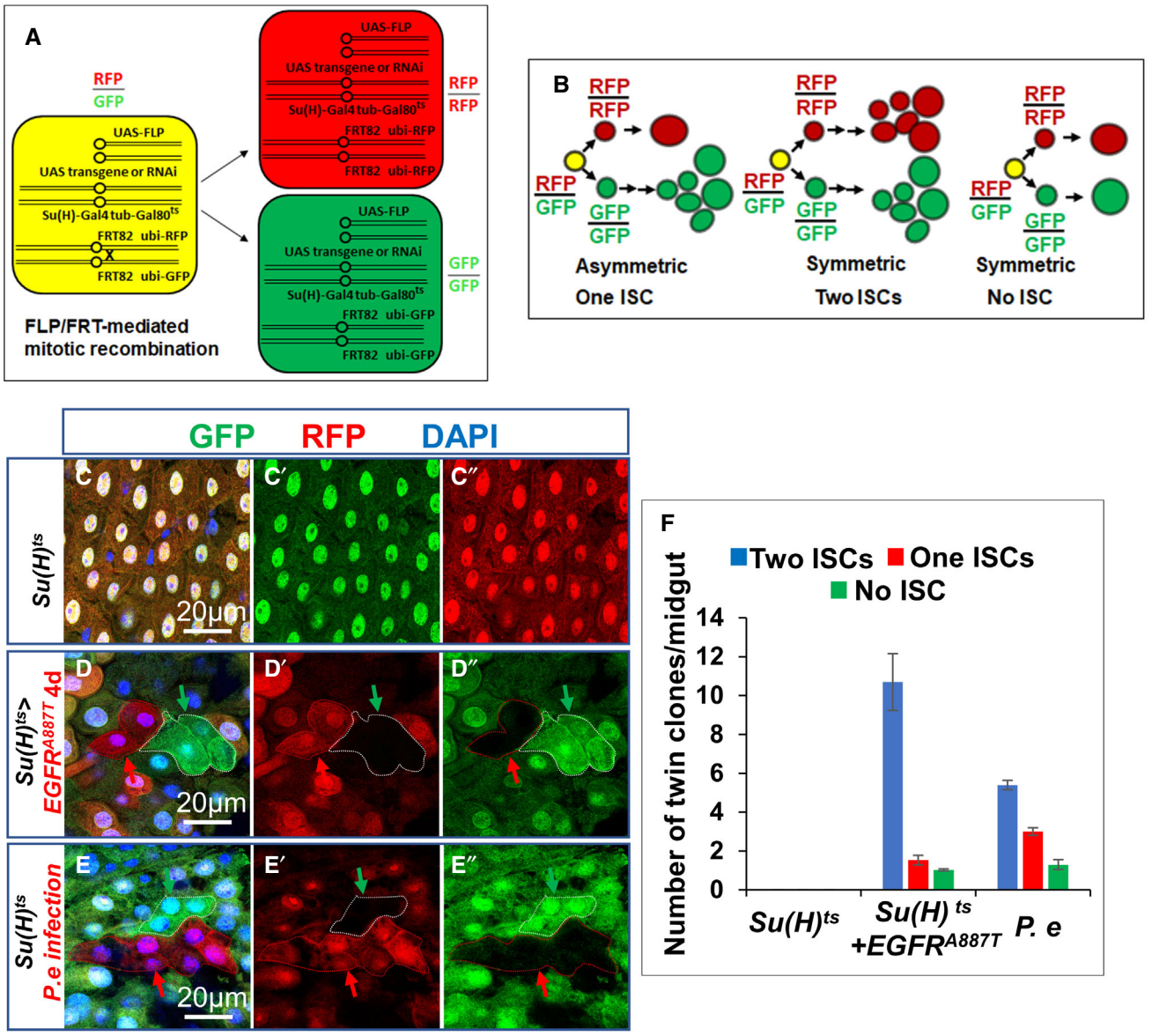

Figure 8. Activating EGFR-Ras signaling in EBs or *P.e.* infection induces EB division to generate two ISCs.

A Schematic drawing of the cell division that produces differentially labeled twin-spot cells (RFP^+ GFP^- and RFP^-GFP^+) through FRT-mediated mitotic recombination. *UAS-Flp* and transgenic overexpression is driven by $Su(H)^{ts}$.

B Schematic drawings of differentially labeled twin-spot clones generated by FLP/FRT-mediated mitotic recombination of dividing cells in EBs.

C–E″ The representative twin clones from midguts when $EGFR^{A887T}$ is overexpressed in EBs (D–D″, red and green arrows) or adult flies were fed with *P.e.* for 36 h (E–E″, red and green arrows), but no twin clone is found in the control (C–C″).

F Quantification of different types of twin clones in the control midguts, or in the midguts with $EGFR^{A887T}$ overexpression or *P.e.* infection. $n = 10$ guts for each genotype.

Data information: Three independent experiments were performed (F).

possibilities about the process of regeneration of ISCs with mitosis. One could be that EBs directly revert to ISCs by direct reprogramming (Higa *et al*, 2022), like induced pluripotent stem cells (Takahashi & Yamanaka, 2006), and then start mitosis. The other one could be that EBs enter mitosis, and then produce ISCs. Our results from immunostaining with Dl support the latter statement, and the two-color lineage tracing experiments further demonstrate that two regenerative ISCs are produced from one EB division, which is distinct from amitosis in the intestine (Lucchetta & Ohlstein, 2017). In addition, we examined expression of genes or activity of signaling pathways for ISC maintenance, such as *esg* (Korzelius *et al*, 2014), Notch signaling (Micchelli & Perrimon, 2006; Ohlstein & Spradling, 2006, 2007), and integrin (Lin *et al*, 2013), in dividing EBs and non-dividing EBs. We found down-regulation of *esg* expression

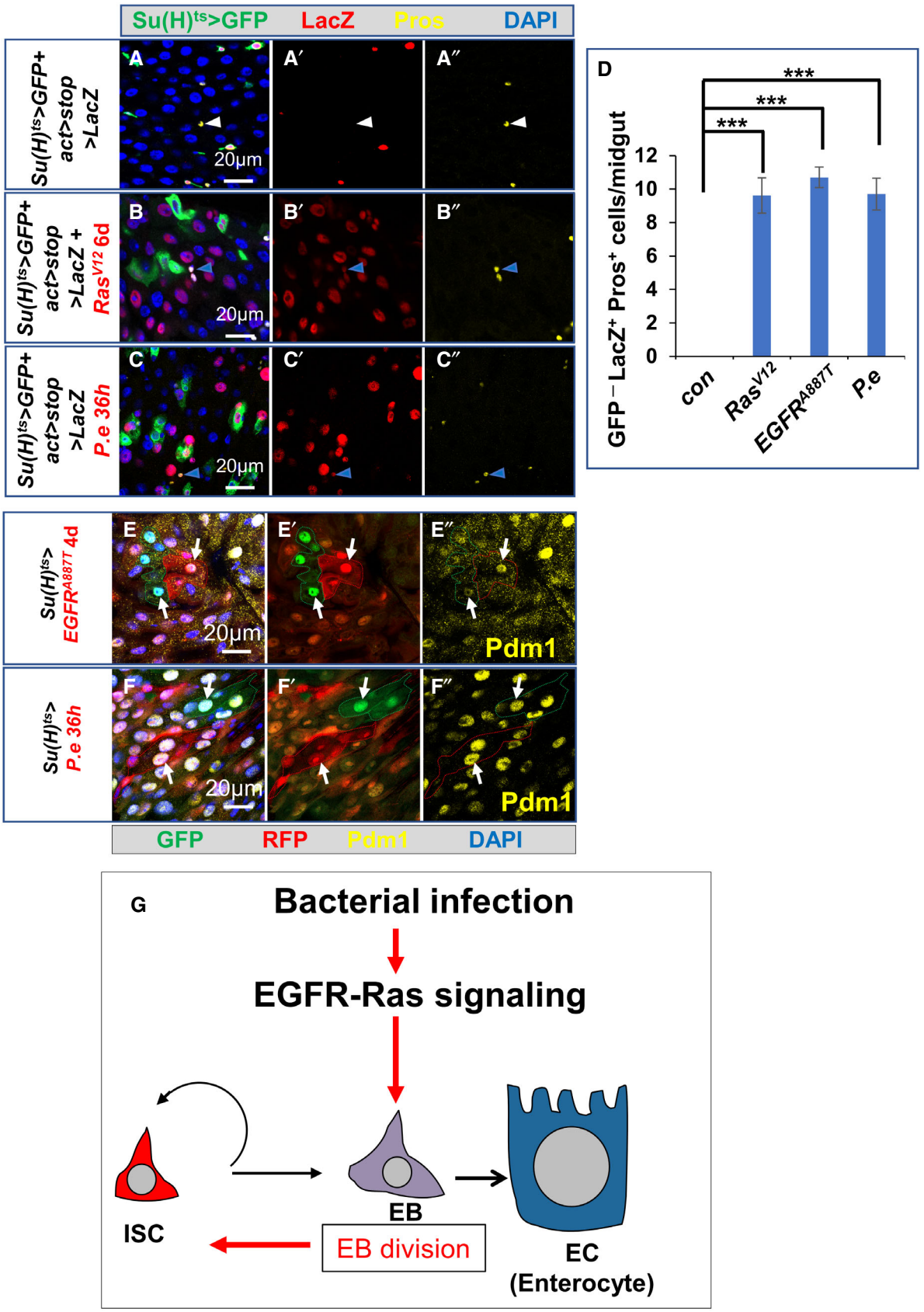

Figure 9.

Figure 9. The regenerative ISCs from EBs can differentiate into mature cells.

A–C″ ISCs from EBs upon Ras^{V12} expression or *P.e.* infection could differentiate to generate EE or pre-EE cells (B-C″, $LacZ^{+}Pros^{+}GFP^{-}$, blue arrowheads), but no EE or pre-EE cells from EBs are found in the control (A–A″, white arrowheads).

D Quantification of EE cells from progenies of EBs with indicated genotypes or treatments. $n = 9$ guts for each genotype or treatment.

E–F″ ECs which were marked by Pdm1 expression were found in pairs of single-color clones (white arrows) in midguts with $EGFR^{A887T}$ expression or upon *P.e.* infection.

G A model for bacterial infection and activation of EGFR-Ras signaling to induce EB mitosis and ISC regeneration.

Data information: Three independent experiments were performed, and error bars are ±SEM. ***$p < 0.001$ (Student's *t*-test) (D).

(Fig EV3A–A‴), but no change in Notch signaling (Fig EV3B and B′) and integrins (Fig EV3D and D′), suggesting no direct reprogramming of EBs. Therefore, activation of EGFR-Ras signaling in EBs which forces EBs to enter the mitotic cycle, together with mitosis, plays a role in the cell fate determination toward ISCs. The replenishment of stem cell pool in mammals is mediated by dedifferentiation, and regeneration of ISCs through mitosis could be another conserved mechanism from *Drosophila* to mammals.

The *Su(H)-Gal4* has been used to mark the EB daughter cells with elevated Notch signaling (Zeng *et al*, 2010). This Gal4 is also used in previous lineage tracing studies to show its expression only in EBs but not in ISCs, and this Gal4-induced lineages include ECs but no EE cells, suggesting the specificity of this Gal4 in labeling EBs in the adult midguts (Biteau & Jasper, 2014; Zeng & Hou, 2015). Resident ISCs are unique in their expression of Dl, but Dl was not detected in the dividing EBs upon bacterial infection or activation of EGFR-Ras signaling, suggesting that these dividing EBs are not ISCs. Therefore, these EBs are referred to as uncommitted EBs, which adopt a fate between the ISCs and EBs. In our lineage tracing experiments, EE cells which are derived from ISCs during normal intestinal development (Biteau & Jasper, 2014; Guo & Ohlstein, 2015; Zeng & Hou, 2015) were identified, indicating that these regenerative ISCs are multipotent. Although we cannot exclude the possibility that these EE cells are generated from EBs with activation of EGFR-Ras signaling or *P.e.* infection, our further experiment with the production of mature ECs from the progenies of regenerative ISCs suggests that the regenerative ISCs from these uncommitted and dividing EBs are multipotent.

Infection of two different Gram-negative bacteria induces the same EB mitosis phenotype, indicating that the immunity signaling pathways might be involved in EB mitosis and/or regeneration of ISCs. The previous studies showed that bacterial infection could induce the IMD pathway in the *Drosophila* intestine (Buchon *et al*, 2009; Zhai *et al*, 2018), but another study reported that Ras/MAPK pathway suppresses IMD in the intestine and fat body (Ragab *et al*, 2011). Therefore, it is unlikely that EGFR-Ras signaling regulates EB mitosis through IMD pathway. Both bacterial infection and activation of EGFR-Ras signaling can activate JAK–STAT pathway in ISCs through up-regulation of ligands to stimulate ISC proliferation (Jiang *et al*, 2009, 2011; Zhai *et al*, 2018). In our studies, noncell-autonomous ISC proliferation was observed when EGFR-Ras signaling was activated in EBs, suggesting that the cytokines of the JAK–STAT pathway could be up-regulated. Indeed, we examined expression of cytokines when EGFR-Ras signaling was activated in EBs and found that *upd3* was up-regulated (Fig EV4). In addition, JAK–STAT signaling was found to be sufficient to induce dedifferentiation of spermatogonia into germline stem cells in the *Drosophila* testis (Brawley & Matunis, 2004). Thus, EGFR-Ras signaling may regulate EB mitosis through the JAK–STAT pathway. To test how specific it is for EGFR-Ras signaling to regulate EB mitosis, we examined several other signaling pathways such as Wnt, Hh, Hippo, and JNK, which can regulate ISC proliferation, we found that activation of Wnt, Hh, and JNK could not induce EB mitosis, and loss of *wts* can stimulate EB mitosis (Fig EV5). Further studies will aid our understanding of the mechanisms underlying intestinal regeneration.

Dysplasia in the mammalian gastrointestinal tract, which is considered as a carcinoma precursor (Li & Jasper, 2016; Pulusu & Lawrance, 2017) and characterized by atypical cellular features, aberrant cell proliferation, and differentiation as well as disorganized architecture, can be mimicked in the *Drosophila* intestine (Micchelli & Perrimon, 2006; Ohlstein & Spradling, 2006; Biteau *et al*, 2008; Apidianakis *et al*, 2009; Jiang *et al*, 2009). Upon bacterial infection, the *Drosophila* intestine undergoes rapid regeneration to replace dying cells and this rapid regeneration can be subverted toward dysplasia (Apidianakis *et al*, 2009; Jiang *et al*, 2009). During regeneration, ISCs with increased proliferation and increased pool size produce more differentiated cells to replace the lost or damaged cells (Apidianakis *et al*, 2009; Jiang *et al*, 2009). Contrary to previous reports, our results indicate that both ISCs and EBs can enter the mitotic cycle, which could make regeneration more efficient. We also find that EBs can generate functional ISCs in response to injury or oncogenic pathway activation, which may contribute to the increased pool of ISCs. Previous studies showed that *Kras* with *Apc* and activation of NF-ƙB (Schwitalla *et al*, 2013) acts as a driving force to promote tumorigenesis by dedifferentiation in mammalian colorectal cancer model (Janssen *et al*, 2006). Therefore, it would be interesting to determine whether the dedifferentiation is mediated by mitosis in mammalian intestines to contribute to tumorigenesis.

Material and Methods

Drosophila genetics and transgenes

Transgenic lines included *UAS-EGFR-RNAi* (VDRC43267), *UAS-*$EGFR^{A887T}$ (BL#9534), *UAS-*Ras^{V12} (Jiang *et al*, 2011), *UAS-Ras-RNAi* (BL#34619), *UAS-*InR^{ACT} (BL#8440), *UAS-stg-RNAi* (BL#34831), *UAS-Flp* (BL#55808), *FRT82Bubi-GFP/CyO*, *FRT82Bubi-RFP/CyO*, *Su(H)-Gal4*, *Su(H)-Gal4 tub-Gal80*^{ts} *UAS-CD8:GFP*, *UAS-FLP; Su(H)-Gal4 tub-Gal80*^{ts} *UAS-CD8:GFP; actP>CD2>LacZ/+*, *esgGal4/UAS-GFP*, *su(H)-Gal80* and *Dl-Gal4*, *tub-Gal80*^{ts} *UAS-GFP*. For feeding experiments with bacteria, Bleomycin (Bleo) or dextran sodium sulfate (DSS), 2–3 days-old female adult flies were used. Flies were cultured in an empty vial containing a piece of chromatography paper (Fisher) wet with 5% (wt/vol) sucrose (Suc) solution as feeding medium (mock treatment) or with *P.e.* or *Ecc15* or 5% DSS or Bleo (25 μg/ml) and 5% (wt/vol) sucrose for one or more days. For experiments with tubGal80^{ts}, the cross with right genotypes were

set up and cultured at 18°C to restrict Gal4 activity. Two- to three-day-old F1 adult flies were shifted to 29°C for the indicated periods of time to inactivate Gal80^{ts} and allow Gal4 to activate UAS transgenes. For bacterial infection with knockdown of genes, flies bearing *Su(H)^{ts}>GFP* or *Su(H)^{ts}>GFP + EGFR-RNAi* (or *Ras-RNAi*) were raised to adults at 18°C, and these adult females were transferred to 29°C for 6 days and then fed with *P.e.* for 36 h. For the lineage tracing experiments with *P.e.* infection, flies bearing *UAS-Flp; Su(H)^{ts}UAS-GFP; actP>stop>LacZ* (or with *UAS-EGFR-RNAi*) were raised to adults at 18°C and then were transferred to 29°C for 6 days and followed by feeding with Suc (control) or *P.e.* for 36 h and normal food for 24 h, and their midguts were immunostained with antibodies against GFP, β-gal and Dl (ISC marker) or Pros (EE marker). For two-color lineage tracing experiments, the cross with right genotypes were set up and cultured at 18°C, and then 3–5-day-old flies expressing *UAS-Flp; Su(H)^{ts}; FRT82BGFP/FRT82BRFP* with or without *UAS-gene* raised in 18°C were transferred to 29°C for the indicated time.

Immunostaining

Female flies were used for gut immunostaining in all experiments. The entire intestine was dissected out and fixed in 1× PBS plus 8% EM-grade paraformaldehyde (Polysciences) for 1 h. Samples were washed and incubated with primary and secondary antibodies in a solution containing 1× PBS, 0.5% BSA, and 0.1% Triton X-100. The following primary antibodies were used: mouse anti-Dl (DSHB), 1:100; rabbit anti-LacZ (MP Biomedicals), 1:1,000; rabbit and mouse anti-PH3 (Millipore), 1:1,000; goat anti-GFP (Abcam), 1:1,000; Mouse anti-Pros (MR1A); Rabbit anti-Pdm1 (gift from X. Yang, Institute of Molecular and Cell Biology, Singapore). Secondary antibodies conjugated to Alexa Fluor 546 donkey anti-mouse and anti-rabbit (Molecular Probes) and Alexa Fluor 633 donkey anti-mouse and anti-rabbit and 488 Donkey anti-goat (Jackson immunoresearch) were used at 1:400. Fluorescently labeled samples were counterstained with DAPI for visualization of DNA. Images were captured with a Zeiss LSM 800 confocal microscope and assembled in Adobe Photoshop.

RT-qPCR

Total RNA was extracted from 10 female guts using Rneasy Plus Mini Kit (74134; Qiagen), and cDNA was synthesized using the iScript cDNA synthesis kit (Bio-Rad). RT-qPCR was performed using iQ SYBR Green System (Bio-Rad). Primer sequences used are: 5′-TCACACATTTAGTGGTGGAAG-3′ and 5′-TTGTGATGCTTGAATTG GTAA-3′ (for *vn*), 5′-CGTGTTTGGCAACAACAAGT-3′ and 5′-TGTG GCAATGCAGTTTAAGG-3′ (for *Krn*), 5′-CGCCCAAGAATGAAAGA GAG-3′ and 5-AGGTATGCTGCTGGTGGAAC-3′ (for *Spi*) and 5′-GAG CACCAAGACTCTGGACA-3′ and 5′-CCAGTGCAACTTGATGTTGC-3′ (for *upd3*). *RpL11* was used as a normalization control. Relative quantification of mRNA levels was calculated using the comparative CT method.

Statistical analyses

Statistical analyses were performed with a two-tailed unpaired *t*-test. *p*-Value is indicated by asterisks in the Figures: $^{**}p < 0.01$; $^{***}p < 0.001$. Differences at $p < 0.01$ were considered significant.

Genotypes for flies in each figure

Figure 1. (B–K′) *Su(H)-Gal4 UAS-CD8:GFP/+*.
Figure 2. (A–C″) *Su(H)-Gal4 UAS-CD8:GFP/+*, (D–F″) *esgGal4/UAS-GFP, su(H)-Gal80*.
Figure 4. (B–C″) *Su(H)-Gal4 UAS-CD8:GFP/+*. (D–E′) *Su(H)-Gal4 tub-Gal80^{ts} UAS-CD8:GFP/+*. (F–H′) *Su(H)-Gal4 tub-Gal80^{ts} UAS-CD8:GFP/UAS-Ras^{V12}*. (I–K′) *Su(H)-Gal4 tub-Gal80^{ts} UAS-CD8:GFP/UAS-EGFR^{A887T}*. (L–N′) *Su(H)-Gal4 tub-Gal80^{ts} UAS-CD8:GFP/UAS-λTop*.
Figure 5. (A–A″) *Su(H)-Gal4 tub-Gal80^{ts} UAS-CD8:GFP/+*. (B–B″) *Su(H)-Gal4 tub-Gal80^{ts} UAS-CD8:GFP/UAS-EGFR^{A887T}*. (C–E) *UAS-Cnn-GFP/+; Dl-Gal4 tub-Gal80^{ts}/+*. (F–H) *UAS-Cnn-GFP/+; Su(H)-Gal4 tub-Gal80^{ts}/UAS-EGFR^{A887T}*. (I–K) *UAS-Cnn-GFP/+; Su(H)-Gal4 tub-Gal80^{ts}/UAS-Ras^{V12}*. (L–N) *UAS-Cnn-GFP/+; Su(H)-Gal4 tub-Gal80^{ts}/+*.
Figure 6. (B–C‴) *UAS-Flp; Su(H)-Gal4 tub-Gal80^{ts} UAS-CD8:GFP; actP>stop>LacZ*.
Figure 7. (A–A″) *UAS-Flp; Su(H)-Gal4 tub-Gal80-Gal4 tub-Gal80^{ts} UAS-CD8:GFP; actP>stop>LacZ*. (B–B‴) *UAS-Flp; Su(H)^{ts} UAS-CD8:GFP/UAS-Ras^{V12}; actP>stop>LacZ*. (C–C‴) *UAS-Flp; Su(H)^{ts} UAS-CD8:GFP/UAS-Ras^{V12}; actP>stop>LacZ/UAS-stg-RNAi*.
Figure 8. (C–C″, E–E″) *UAS-Flp; Su(H)-Gal4 tub-Gal80^{ts}; FRT82BGFP/FRT82BRFP*. (D–D″) *UAS-Flp; Su(H)-Gal4 tub-Gal80^{ts}/UAS-EGFR^{A887T}; FRT82BGFP/ FRT82BRFP*.
Figure 9. (A–A″, C–C″) *UAS-Flp; Su(H)-Gal4 tub-Gal80^{ts} UAS-CD8:GFP; actP>stop>LacZ*. (B-B″) *UAS-Flp; Su(H)-Gal4 tub-Gal80^{ts} UAS-CD8:GFP/UAS-Ras^{V12}; actP>stop>LacZ*. (E–E″) *UAS-Flp; Su(H)-Gal4 tub-Gal80^{ts}/UAS-EGFR^{A887T}; FRT82BGFP/FRT82BRFP*. (F–F″) *UAS-Flp; Su(H)-Gal4 tub-Gal80^{ts}; FRT82BGFP/FRT82BRFP*.

Genotypes for flies in each supplementary figure

Figure EV1. (A) *Su(H)-Gal4 UAS-CD8:GFP/+*. (B) *Su(H)-Gal4 tub-Gal80^{ts} UAS-CD8:GFP/+; UAS-stg-RNAi/+*. (C) *Su(H)-Gal4 tub-Gal80^{ts} UAS-CD8:GFP/+; UAS-InR^{ACT}/+*.
Figure EV2. *UAS-Flp; Su(H)-Gal4 tub-Gal80^{ts}/UAS-EGFR^{A887T}; FRT82BGFP/FRT82BRFP*.
Figure EV3. (A–A‴) *Su(H)-Gal4/UAS-GFP; esg-lacZ*. (B) *E(spl)mb-CD2; Su(H)-Gal4-UAS-CD8:GFP*. (C–D′) *Su(H)-Gal4-UAS-CD8:GFP*.
Figure EV4. *Su(H)-Gal4 tub-Gal80^{ts} UAS-CD8:GFP/UAS-EGFR^{A887T}*.
Figure EV5. *Su(H)-Gal4 tub-Gal80^{ts} UAS-CD8:GFP; UAS-wts-RNAi*.

Data availability

No data amenable to database repository deposition were generated in this study.

Expanded View for this article is available online.

Acknowledgements
The authors thank Bloomington *Drosophila* Stock Center (NIH P400D018537), VDRC and Developmental Studies Hybridoma Bank for providing fly lines and antibodies, and thank Professors Yiping Chen, SM Jazwinski, Vivian Fonseca, Hong Liu, and Jun-yuan Ji at Tulane University for discussion. This work was supported by the National Institutes of Health (grant P20GM103629 to AT; grant GM072562, CA224381 and CA227789 to WMD; GM118063 to JJ), Carol

Lavin Bernick Faculty Grant (AT), Bridge Research Fund at Tulane University (AT), Bridge Research Fund at School of Medicine of Tulane University (AT), and Welch foundation grant (I-1603) to JJ.

Author contributions

Aiguo Tian: Conceptualization; data curation; formal analysis; supervision; funding acquisition; investigation; methodology; writing – original draft; project administration; writing – review and editing. **Virginia Morejon:** Methodology; writing – review and editing. **Sarah Kohoutek:** Methodology; writing – review and editing. **Yi-Chun Huang:** Methodology. **Wu-Min Deng:** writing – review and editing. **Jin Jiang:** writing – review and editing.

Disclosure and competing interests statement

The authors declare that they have no conflict of interest.

References

Amcheslavsky A, Jiang J, Ip YT (2009) Tissue damage-induced intestinal stem cell division in *Drosophila*. *Cell Stem Cell* 4: 49 – 61

Apidianakis Y, Pitsouli C, Perrimon N, Rahme L (2009) Synergy between bacterial infection and genetic predisposition in intestinal dysplasia. *Proc Natl Acad Sci USA* 106: 20883 – 20888

Barker N, van Es JH, Kuipers J, Kujala P, van den Born M, Cozijnsen M, Haegebarth A, Korving J, Begthel H, Peters PJ *et al* (2007) Identification of stem cells in small intestine and colon by marker gene Lgr5. *Nature* 449: 1003 – 1007

Beehler-Evans R, Micchelli CA (2015) Generation of enteroendocrine cell diversity in midgut stem cell lineages. *Development* 142: 654 – 664

Beumer J, Clevers H (2016) Regulation and plasticity of intestinal stem cells during homeostasis and regeneration. *Development* 143: 3639 – 3649

Biteau B, Jasper H (2011) EGF signaling regulates the proliferation of intestinal stem cells in *Drosophila*. *Development* 138: 1045 – 1055

Biteau B, Jasper H (2014) Slit/Robo signaling regulates cell fate decisions in the intestinal stem cell lineage of drosophila. *Cell Rep* 7: 1867 – 1875

Biteau B, Hochmuth CE, Jasper H (2008) JNK activity in somatic stem cells causes loss of tissue homeostasis in the aging drosophila gut. *Cell Stem Cell* 3: 442 – 455

Biteau B, Hochmuth CE, Jasper H (2011) Maintaining tissue homeostasis: dynamic control of somatic stem cell activity. *Cell Stem Cell* 9: 402 – 411

Brawley C, Matunis E (2004) Regeneration of male germline stem cells by spermatogonial dedifferentiation *in vivo*. *Science* 304: 1331 – 1334

Buchon N, Broderick NA, Poidevin M, Pradervand S, Lemaitre B (2009) Drosophila intestinal response to bacterial infection: activation of host defense and stem cell proliferation. *Cell Host Microbe* 5: 200 – 211

Buchon N, Broderick NA, Kuraishi T, Lemaitre B (2010) *Drosophila* EGFR pathway coordinates stem cell proliferation and gut remodeling following infection. *BMC Biol* 8: 152

Chen J, Xu N, Wang C, Huang P, Huang H, Jin Z, Yu Z, Cai T, Jiao R, Xi R (2018) Transient Scute activation via a self-stimulatory loop directs enteroendocrine cell pair specification from self-renewing intestinal stem cells. *Nat Cell Biol* 20: 152 – 161

van Es JH, Sato T, van de Wetering M, Lyubimova A, Yee Nee AN, Gregorieff A, Sasaki N, Zeinstra L, van den Born M, Korving J *et al* (2012) Dll1+ secretory progenitor cells revert to stem cells upon crypt damage. *Nat Cell Biol* 14: 1099 – 1104

Gabay L, Seger R, Shilo BZ (1997) MAP kinase *in situ* activation atlas during *Drosophila* embryogenesis. *Development* 124: 3535 – 3541

Germani F, Bergantinos C, Johnston LA (2018) Mosaic analysis in *Drosophila*. *Genetics* 208: 473 – 490

Golic KG, Lindquist S (1989) The FLP recombinase of yeast catalyzes site-specific recombination in the *Drosophila* genome. *Cell* 59: 499 – 509

Goulas S, Conder R, Knoblich JA (2012) The par complex and integrins direct asymmetric cell division in adult intestinal stem cells. *Cell Stem Cell* 11: 529 – 540

Guo Z, Ohlstein B (2015) Stem cell regulation. Bidirectional notch signaling regulates drosophila intestinal stem cell multipotency. *Science* 350: aab0988

Higa T, Okita Y, Matsumoto A, Nakayama S, Oka T, Sugahara O, Koga D, Takeishi S, Nakatsumi H, Hosen N *et al* (2022) Spatiotemporal reprogramming of differentiated cells underlies regeneration and neoplasia in the intestinal epithelium. *Nat Commun* 13: 1500

Hung RJ, Hu Y, Kirchner R, Liu Y, Xu C, Comjean A, Tattikota SG, Li F, Song W, Ho Sui S *et al* (2020) A cell atlas of the adult drosophila midgut. *Proc Natl Acad Sci USA* 117: 1514 – 1523

Janssen KP, Alberici P, Fsihi H, Gaspar C, Breukel C, Franken P, Rosty C, Abal M, El Marjou F, Smits R *et al* (2006) APC and oncogenic KRAS are synergistic in enhancing Wnt signaling in intestinal tumor formation and progression. *Gastroenterology* 131: 1096 – 1109

Jiang H, Edgar BA (2012) Intestinal stem cell function in *Drosophila* and mice. *Curr Opin Genet Dev* 22: 354 – 360

Jiang H, Patel PH, Kohlmaier A, Grenley MO, McEwen DG, Edgar BA (2009) Cytokine/Jak/Stat signaling mediates regeneration and homeostasis in the *Drosophila* midgut. *Cell* 137: 1343 – 1355

Jiang H, Grenley MO, Bravo MJ, Blumhagen RZ, Edgar BA (2011) EGFR/Ras/MAPK signaling mediates adult midgut epithelial homeostasis and regeneration in *Drosophila*. *Cell Stem Cell* 8: 84 – 95

Jiang H, Tian A, Jiang J (2016) Intestinal stem cell response to injury: lessons from *Drosophila*. *Cell Mol Life Sci* 73: 3337 – 3349

Jones JC, Brindley CD, Elder NH, Myers MG Jr, Rajala MW, Dekaney CM, McNamee EN, Frey MR, Shroyer NF, Dempsey PJ (2019) Cellular plasticity of Defa4(Cre)-expressing Paneth cells in response to notch activation and intestinal injury. *Cell Mol Gastroenterol Hepatol* 7: 533 – 554

Karim FD, Rubin GM (1998) Ectopic expression of activated Ras1 induces hyperplastic growth and increased cell death in drosophila imaginal tissues. *Development* 125: 1 – 9

Karpowicz P, Perez J, Perrimon N (2010) The hippo tumor suppressor pathway regulates intestinal stem cell regeneration. *Development* 137: 4135 – 4145

Kohlmaier A, Fassnacht C, Jin Y, Reuter H, Begum J, Dutta D, Edgar BA (2015) Src kinase function controls progenitor cell pools during regeneration and tumor onset in the drosophila intestine. *Oncogene* 34: 2371 – 2384

Korzelius J, Naumann SK, Loza-Coll MA, Chan JS, Dutta D, Oberheim J, Glasser C, Southall TD, Brand AH, Jones DL *et al* (2014) Escargot maintains stemness and suppresses differentiation in drosophila intestinal stem cells. *EMBO J* 33: 2967 – 2982

Lesokhin AM, Yu SY, Katz J, Baker NE (1999) Several levels of EGF receptor signaling during photoreceptor specification in wild-type, ellipse, and null mutant drosophila. *Dev Biol* 205: 129 – 144

Li H, Jasper H (2016) Gastrointestinal stem cells in health and disease: from flies to humans. *Dis Model Mech* 9: 487 – 499

Lin G, Xu N, Xi R (2008) Paracrine wingless signalling controls self-renewal of *Drosophila* intestinal stem cells. *Nature* 455: 1119 – 1123

Lin G, Zhang X, Ren J, Pang Z, Wang C, Xu N, Xi R (2013) Integrin signaling is required for maintenance and proliferation of intestinal stem cells in *Drosophila*. *Dev Biol* 377: 177 – 187

Lucchetta EM, Ohlstein B (2017) Amitosis of Polyploid cells regenerates functional stem cells in the drosophila intestine. *Cell Stem Cell* 20: e606

Micchelli CA, Perrimon N (2006) Evidence that stem cells reside in the adult *Drosophila* midgut epithelium. *Nature* 439: 475 – 479

Murata K, Jadhav U, Madha S, van Es J, Dean J, Cavazza A, Wucherpfennig K, Michor F, Clevers H, Shivdasani RA (2020) Ascl2-dependent cell dedifferentiation drives regeneration of ablated intestinal stem cells. *Cell Stem Cell* 26: 377 – 390.e6

O'Brien LE, Soliman SS, Li X, Bilder D (2011) Altered modes of stem cell division drive adaptive intestinal growth. *Cell* 147: 603 – 614

Ohlstein B, Spradling A (2006) The adult *Drosophila* posterior midgut is maintained by pluripotent stem cells. *Nature* 439: 470 – 474

Ohlstein B, Spradling A (2007) Multipotent drosophila intestinal stem cells specify daughter cell fates by differential notch signaling. *Science* 315: 988 – 992

Pulusu SSR, Lawrance IC (2017) Dysplasia and colorectal cancer surveillance in inflammatory bowel disease. *Expert Rev Gastroenterol Hepatol* 11: 711 – 722

Queenan AM, Ghabrial A, Schupbach T (1997) Ectopic activation of torpedo/Egfr, a *Drosophila* receptor tyrosine kinase, dorsalizes both the eggshell and the embryo. *Development* 124: 3871 – 3880

Ragab A, Buechling T, Gesellchen V, Spirohn K, Boettcher AL, Boutros M (2011) *Drosophila* Ras/MAPK signalling regulates innate immune responses in immune and intestinal stem cells. *EMBO J* 30: 1123 – 1136

Ren F, Wang B, Yue T, Yun EY, Ip YT, Jiang J (2010) Hippo signaling regulates drosophila intestine stem cell proliferation through multiple pathways. *Proc Natl Acad Sci USA* 107: 21064 – 21069

Ren F, Shi Q, Chen Y, Jiang A, Ip YT, Jiang H, Jiang J (2013) *Drosophila* Myc integrates multiple signaling pathways to regulate intestinal stem cell proliferation during midgut regeneration. *Cell Res* 23: 1133 – 1146

Sansonetti PJ (2004) War and peace at mucosal surfaces. *Nat Rev Immunol* 4: 953 – 964

Schmitt M, Schewe M, Sacchetti A, Feijtel D, van de Geer WS, Teeuwssen M, Sleddens HF, Joosten R, van Royen ME, van de Werken HJG *et al* (2018) Paneth cells respond to inflammation and contribute to tissue regeneration by acquiring stem-like features through SCF/c-kit signaling. *Cell Rep* 24: 2312 – 2328.e7

Schwitalla S, Fingerle AA, Cammareri P, Nebelsiek T, Goktuna SI, Ziegler PK, Canli O, Heijmans J, Huels DJ, Moreaux G *et al* (2013) Intestinal tumorigenesis initiated by dedifferentiation and acquisition of stem-cell-like properties. *Cell* 152: 25 – 38

Shaw RL, Kohlmaier A, Polesello C, Veelken C, Edgar BA, Tapon N (2010) The hippo pathway regulates intestinal stem cell proliferation during drosophila adult midgut regeneration. *Development* 137: 4147 – 4158

Staley BK, Irvine KD (2010) Warts and Yorkie mediate intestinal regeneration by influencing stem cell proliferation. *Curr Biol* 20: 1580 – 1587

Takahashi K, Yamanaka S (2006) Induction of pluripotent stem cells from mouse embryonic and adult fibroblast cultures by defined factors. *Cell* 126: 663 – 676

Tetteh PW, Basak O, Farin HF, Wiebrands K, Kretzschmar K, Begthel H, van den Born M, Korving J, de Sauvage F, van Es JH *et al* (2016) Replacement of lost Lgr5-positive stem cells through plasticity of their enterocyte-lineage daughters. *Cell Stem Cell* 18: 203 – 213

Tian A, Jiang J (2014) Intestinal epithelium-derived BMP controls stem cell self-renewal in drosophila adult midgut. *Elife* 3: e01857

Tian A, Shi Q, Jiang A, Li S, Wang B, Jiang J (2015) Injury-stimulated hedgehog signaling promotes regenerative proliferation of *Drosophila* intestinal stem cells. *J Cell Biol* 208: 807 – 819

Tian A, Wang B, Jiang J (2017) Injury-stimulated and self-restrained BMP signaling dynamically regulates stem cell pool size during *Drosophila* midgut regeneration. *Proc Natl Acad Sci USA* 114: E2699 – E2708

Willms RJ, Zeng J, Campbell SD (2020) Myt1 kinase couples mitotic cell cycle exit with differentiation in *Drosophila*. *Cell Rep* 33: 108400

Yu S, Tong K, Zhao Y, Balasubramanian I, Yap GS, Ferraris RP, Bonder EM, Verzi MP, Gao N (2018) Paneth cell multipotency induced by notch activation following injury. *Cell Stem Cell* 23: 46 – 59.e5

Zeng X, Hou SX (2015) Enteroendocrine cells are generated from stem cells through a distinct progenitor in the adult *Drosophila* posterior midgut. *Development* 142: 644 – 653

Zeng X, Chauhan C, Hou SX (2010) Characterization of midgut stem cell- and enteroblast-specific Gal4 lines in drosophila. *Genesis* 48: 607 – 611

Zhai Z, Boquete JP, Lemaitre B (2018) Cell-specific Imd-NF-kappaB responses enable simultaneous antibacterial immunity and intestinal epithelial cell shedding upon bacterial infection. *Immunity* 48: e897

Zwick RK, Ohlstein B, Klein OD (2019) Intestinal renewal across the animal kingdom: comparing stem cell activity in mouse and drosophila. *Am J Physiol Gastrointest Liver Physiol* 316: G313 – G322